Pergamon

Int. J. Solids Structures Vol. 32, No. 20, pp. 2967–1987, 1995

0020–7683/95 $9.50 + .00

0020–7683(94)00302–5

AN INCREMENTAL ELASTIC–VISCOPLASTIC THEORY INDICATING A REDUCED MODULUS FOR NON-PROPORTIONAL BUCKLING

M. B. RUBIN and S. R. BODNER
Faculty of Mechanical Engineering, Technion—Israel Institute of Technology, 32000 Haifa, Israel

(*Received* 17 *May* 1994; *in revised form* 17 *October* 1994)

Abstract—The small deformation elastic–viscoplastic constitutive equations of Bodner–Partom are modified to model strong non-proportional loading paths such as experienced in corner turning tests and certain cases of inelastic buckling. An essential generalization is made to the flow rule, causing the magnitude and direction of plastic strain rate to become an explicit function of deviatoric total strain rate as well as of stress and hardening variables. With this and other modifications, the equations indicate some of the important characteristics of the response to abrupt changes in the loading direction. These are: (a) a reduced effective shear modulus; (b) a transient drop in the effective stress; and (c) a transient non-coaxiality of the plastic strain rate relative to the deviatoric stress. Predictions of the modified theory compare reasonably well with experimental values for inelastic torsional buckling of axially compressed cruciform columns and for corner turning tests.

1. INTRODUCTION

Theories of plastic deformation are intended to apply for all loading conditions. However, some cases of non-proportional loading where the ratios of the stress components, and also those of strain rate, are not constant seem to offer special difficulties. As examples, the classical incremental theory of plasticity does not adequately predict the material response to a rapid change in the direction of imposed straining, e.g. a corner turning test, nor does that theory indicate realistic bifurcation loads should buckling initiate abrupt changes in the relative proportions of the stress components.

Buckling in the plastic range has been traditionally treated by retaining elastic buckling formulae in which effective or reduced moduli are utilized. For example, Shanley (1947), following Engesser (1889), argued on the basis that elastic unloading would not occur that the governing modulus for bifurcation buckling of columns in bending is the tangent to the stress–strain curve at the applied stress level. The general bifurcation theory of Hill for rate independent plasticity indicates that under the condition of continuous loading, bifurcation is controlled by the instantaneous moduli of the elastic–plastic stress–strain relation. Also, the formulae presented in a table by Stowell (1948: p. 2) and the writings of a number of other investigators suggest that the reduced modulus for buckling in the plastic range depends on the buckling mode and hence on the direction of straining at the onset of buckling.

An essential difficulty in the treatment of plastic buckling is the determination of controlling moduli for test configurations that exhibit non-proportional loading paths at the onset of buckling (compared to the initial state). To obtain agreement with test data, various investigators have expressed these moduli as functions of the tangent and secant moduli as well as the elastic moduli, e.g. Gerard and Becker (1957). The secant modulus was indicated by Stowell (1951) to be relevant for cruciform columns that buckle in torsion and also by Gerard (1946) and others for plate buckling and various shell buckling situations. Paradoxically, these test results are not properly predicted by incremental theory of plasticity associated with a standard yield surface, whereas the generally inapplicable deformation theory seems to supply reasonable results. This subject is thoroughly discussed by Hutchinson (1974) in his extensive review of plastic buckling. The discrepancy is particularly demonstrated in the case of inelastic torsional buckling of axially compressed cruciform columns, where the loading path can be approximated by a 90° corner turning test. For this case, incremental theory predicts elastic buckling while the test results seem to correspond to the secant modulus in accord with deformation theory. Deformation theory would also supply the tangent modulus for bifurcation buckling of columns in bending.

A number of investigators have pointed to the need for the shear modulus to be reduced from the elastic value for multiaxial stress cases where shear strains and stresses generated at buckling were zero prior to buckling. Bushnell (1976) suggests use of the secant modulus in shear in the otherwise incremental plastic flow formulation of the BOSOR5 numerical program for buckling of plates and shells. Recent suggestions of this type have also been made by Inoue and Kato (1993), and Inoue (1994).

Attempts to improve the predictive capability of incremental plasticity theory have followed two directions. One is to modify the basic formulation of the particular problem to consider factors such as initial imperfections and more realistic boundary conditions, e.g. the works of Onat and Drucker (1953), Gjelsvik and Lin (1987), and Tugcu (1991). Those considerations would lead to the pre-buckling state containing the stress components that are generated at buckling so that the relative non-proportionality of those components at buckling would be reduced. The other method is to modify the smooth yield surface of standard incremental theory to admit the formation of corners (vertices) at the loading point. This approach [e.g. Christoffersen and Hutchinson (1979)] permits the generation of a wider range of strain rate components corresponding to non-coaxiality of plastic strain rate and deviatoric stress at buckling. The connection between deformation theory and an incremental theory in which vertices can develop at the load point of the yield surface has been discussed by Budiansky (1959) and Hutchinson (1974). However, full experimental support of the existence of corners is lacking and the situation is still unclear. A more recent review of the subject and exercises that combine the two approaches is contained in the paper by Needleman and Tvergaard (1982).

In the present paper, an alternative procedure based on modification of the plastic flow law is proposed which leads to a reduced shear modulus for non-proportional buckling paths. The formulation relies on the small strain, "unified" elastic–viscoplastic theory of Bodner–Partom (B-P) (1972, 1975) which does not require a yield surface or loading/unloading conditions. That theory was initially developed for proportional loading conditions but has been modified to account for multiaxial directional hardening and various non-proportional loading effects such as additional hardening associated with that loading (Bodner, 1985, 1987). Unlike most other formulations, the B-P theory does not rely on "back stress" parameters and treats reversed loading by introducing a scalar effective value of a directional hardening tensor. For convenience, the B-P theory is briefly summarized in Section 3.

Two generalizations of the B-P theory are proposed. The first generalization, which is presented in Section 4, shows that it is possible to develop an incremental theory which indicates a reduced effective shear modulus for non-proportional buckling paths. The main idea associated with this generalization is the assumption that the direction of the plastic strain rate depends explicitly on the deviatoric total strain rate as well as on stress, temperature, and history dependent hardening variables. The governing viscoplastic flow rule is then essentially different from the usual constitutive equations for plastic strain rate which are independent of the total strain rate. It therefore follows that the present formulation is not included in the class of theories analysed by Tvergaard (1988) who, among others, has shown that bifurcation buckling of elastic–viscoplastic structures would be elastic for constitutive models of the standard form.

Specifically, we assume that the direction of the plastic strain rate depends not only on the deviatoric stress but also on another deviatoric tensor, that is the component of the deviatoric total strain rate normal to the deviatoric stress. That term also contains an additional parameter which depends on the hardening variables and influences the magnitude of the reduced effective shear modulus for corner turning tests. This modification produces realistic values of the reduced effective shear modulus for non-proportional buckling paths as well as non-coaxiality of the deviatoric stress and the plastic strain rate.

Since the reduced effective modulus for buckling is sensitive to changes in the direction of loading at the onset of buckling, important information about the material response under such situations can be studied using well controlled corner turning tests. Experiments of corner turning tests have been conducted by various groups of Japanese investigators in the 1970s and early 1980s [e.g. Ohashi and Ohno (1982)], who observed non-coaxiality of plastic strain rate and deviatoric stress and a significant drop in effective stress at the change in the direction of straining. However, they did not suggest the relevance of their studies to buckling problems. Simulations of these corner turning tests using the modified equations of Section 4 indicated the drop of von Mises effective stress, but the value obtained was too small. In order to enhance this drop, the theory was further modified in Section 5.

Since the rate-dependent theory developed in Sections 4 and 5 predicts nearly rate-independent response when one of the parameters, n, becomes large, an attempt was made to develop an associated rate-independent theory which uses a yield surface. The theoretical difficulties with such a rate-independent theory discussed in Section 6 emphasize the importance of the rate-dependent nature of the viscoplastic theory used here as a basis for the modifications of Sections 4 and 5.

In the following section, a discussion is presented of the experiments reported by Stowell (1951) on plastic buckling of cruciform columns and the corner turning tests of Ohashi and Ohno (1982). The B-P theory is briefly summarized in Section 3, and the essential modifications of the theory are described in Sections 4 and 5. Also, Section 6 discusses some of the difficulties encountered with an associated rate-independent theory which uses a yield surface. The modified equations of Section 5, which include the changes introduced in Section 4, are capable of modeling three main effects observed in corner turning tests: a reduced effective shear modulus, non-coaxiality between the plastic strain rate and the deviatoric stress, and the transient drop in effective stress. As a consequence, these constitutive equations should be capable of analysing bifurcation buckling and also post-buckling behavior to the limits of applicability of a small strain material model.

2. DISCUSSION OF EXPERIMENTS

In order to critically discuss the work of Stowell (1951) on buckling of columns with a cruciform shaped cross-section, it is convenient to recall some basic equations associated with the incremental theory of plasticity. To this end, attention is confined to the small strain (displacement) purely mechanical theory and let: $\boldsymbol{\sigma}$ denote the stress, p the pressure, $\boldsymbol{\sigma}'$ the deviatoric stress, $\boldsymbol{\varepsilon}$ the total strain, $\boldsymbol{\varepsilon}'$ the deviatoric total strain, and $\boldsymbol{\varepsilon}_p$ the plastic strain which is deviatoric due to plastic incompressibility. Here, the usual form of Hooke's law for isotropic elastic response is retained, so that

$$\boldsymbol{\sigma} = -p\mathbf{I}+\boldsymbol{\sigma}', \tag{1a}$$

$$p = -k(\boldsymbol{\varepsilon}\cdot\mathbf{I}), \quad \boldsymbol{\sigma}' = 2G(\boldsymbol{\varepsilon}'-\boldsymbol{\varepsilon}_p), \tag{1b,c}$$

where $\mathbf{I}$ is the unit tensor, k is the bulk modulus, G is the shear modulus, and the notation $\mathbf{A}\cdot\mathbf{B} = \mathrm{tr}\,(\mathbf{A}\mathbf{B}^T)$ denotes the inner product between two second order tensors $\mathbf{A}$, $\mathbf{B}$. Also, the von Mises effective stress σ_{eff} and the effective deviatoric total strain $\varepsilon_{\mathrm{eff}}$ are defined by

$$\sigma_{\mathrm{eff}}^2 = \tfrac{3}{2}\boldsymbol{\sigma}'\cdot\boldsymbol{\sigma}', \quad \varepsilon_{\mathrm{eff}}^2 = \tfrac{2}{3}\boldsymbol{\varepsilon}'\cdot\boldsymbol{\varepsilon}'. \tag{2a,b}$$

Furthermore, the accumulated deviatoric total strain S for general loading paths is defined by integrating the equation

$$\dot{S} = (\tfrac{2}{3})^{1/2}|\dot{\boldsymbol{\varepsilon}}'|, \tag{3}$$

where a superposed dot means time differentiation and the notation $|\mathbf{A}| = \sqrt{\mathbf{A}\cdot\mathbf{A}}$ is the magnitude of the tensor $\mathbf{A}$.

As a consequence of plastic incompressibility, the volumetric response (1b) remains elastic so that plasticity can only effect the direction and magnitude of the deviatoric stress (1c). This means that when searching for an appropriate reduced modulus for plastic buckling, it is convenient to write the elastic buckling criteria in terms of the moduli k and G. Then the reduced modulus is assumed to be determined by the elastic formula with G replaced by $\bar{G}$. For example, the elastic torsional buckling analysis of the cruciform column developed by Stowell (1951: eqn A33) gives the critical stress σ_{cr} for the onset of elastic buckling,

$$\sigma_{cr} = G\left[\left(\frac{t}{b}\right)^2 + \left(\frac{1}{1+\frac{G}{3k}}\right)\left(\frac{\pi t}{L}\right)^2\right], \tag{4}$$

where L is the length of the cruciform column, which is composed of four identical flanges, each having width b and thickness t.

For plastic buckling, it is assumed that formula (4) still holds with σ_{cr} replaced by the experimental value σ^*_{cr} of the critical stress, G replaced by its reduced value $\bar{G}$, and with k remaining unchanged, so that

$$\sigma^*_{cr} = \bar{G}\left[\left(\frac{t}{b}\right)^2 + \left(\frac{1}{1+\frac{\bar{G}}{3k}}\right)\left(\frac{\pi t}{L}\right)^2\right]. \tag{5}$$

Here, it is tacitly assumed that relationships between the reduced values of the elastic constants remain the same as those of the actual elastic constants so that the reduced value $\bar{E}$ of Young's modulus E and the increased value $\bar{\nu}$ of Poisson's ratio ν are related to $\bar{G}$ and k by the formulae

$$\frac{1}{\bar{E}} = \frac{1}{3\bar{G}} + \frac{1}{9k}, \quad \bar{\nu} = \frac{1}{2}\left[\frac{1-\frac{2\bar{G}}{3k}}{1+\frac{\bar{G}}{3k}}\right]. \tag{6a,b}$$

Thus, as $\bar{G}$ becomes small relative to $3k$, the value of $\bar{E}$ approaches $3\bar{G}$, and the value of $\bar{\nu}$ approaches 1/2, as to be expected. In this regard, the problem of predicting the critical stress for plastic buckling reduces to the problem of predicting the appropriate value of the reduced shear modulus $\bar{G}$.

Given values of the geometry of the column $\{t/b, b/L\}$, the elastic constants, and the measured value σ^*_{cr} of the critical stress from the experimental data for buckling, Gerard and Becker (1957) used formula (4) to determine the elastic value of critical stress and defined the normalized experimental buckling stress η by

$$\eta = \frac{\sigma^*_{cr}}{\sigma_{cr}}. \tag{7}$$

Alternatively, the quadratic equation resulting from eqn (5) for the value of the reduced shear modulus $\bar{G}$ can be solved to obtain

$$\bar{G} = \frac{3k}{2}\left[r + \left\{r^2 + 4\left(\frac{\sigma^*_{cr}}{3k}\right)\left(\frac{b}{t}\right)^2\right\}^{1/2}\right], \tag{8}$$

where r is defined by

$$r = \left(\frac{\sigma_{cr}^*}{3k}\right)\left(\frac{b}{t}\right)^2 - 1 - \left(\frac{\pi b}{L}\right)^2, \tag{9}$$

and the appropriate sign of the solution is chosen so that eqn (8) predicts the correct limiting value when b/L is negligible. In analysing experimental data of plastic buckling, it is common to assume that the increased value $\bar{\nu}$ of Poisson's ratio is 1/2 [Stowell (1948: p. 2)]. This approximation is equivalent to taking $\bar{G}/k$ equal to zero in eqn (5) so that the approximate value $\bar{G}_1$ of $\bar{G}$ is given by

$$\bar{G}_1 = \frac{\sigma_{cr}^*\left(\frac{b}{t}\right)^2}{1+\left(\frac{\pi b}{L}\right)^2}. \tag{10}$$

Another approximation [Hutchinson (1974: p. 100)] is to neglect the term b/L in eqn (10) to obtain the approximate value $\bar{G}_2$ of $\bar{G}$ given by

$$\bar{G}_2 = \sigma_{cr}^*\left(\frac{b}{t}\right)^2. \tag{11}$$

The material used in the experiments of Stowell (1951) was 24S-T4 extruded aluminum which is more commonly known today as 2024-T4 aluminum. The handbook edited by Gray (1957) indicates that the elastic constants of many aluminum alloys are reasonably uniform so here we take $\nu = 1/3$ and specify a consistent set of elastic constants by

$$k = 71.0\,\text{GPa}, \quad E = 71.0\,\text{GPa}, \tag{12a,b}$$

$$G = 26.6\,\text{GPa}, \quad \nu = \tfrac{1}{3}. \tag{12c,d}$$

Using this value of k together with the experimental data supplied by Stowell (1951: p. 5), it is possible to obtain values for η and the normalized values of $\bar{G}$, $\bar{G}_1$, and $\bar{G}_2$ [associated with eqns (7), (8), (10) and (11), respectively] which are given in Table 1. It is noted that the values of η and the normalized values of $\bar{G}$ are nearly identical, which means that the terms in square brackets in eqns (4) and (5) are very similar. From Table 1, the error caused by neglecting the effect of the length of the column ($\bar{G}_2$) is significant, but the error caused by assuming that the material is fully incompressible ($\bar{G}_1$) is less than 4%.

Table 1. Experimental data [Stowell (1951: p. 5)] and reduced moduli for inelastic torsional buckling of a cruciform section column

b/t	L/b	σ_{cr}^* (GPa)	η	$\bar{G}/G$	$\bar{G}_1/G$	$\bar{G}_2/G$
8	12	0.316	0.717	0.715	0.711	0.760
9	18	0.280	0.830	0.830	0.828	0.853
10	4	0.309	0.750	0.743	0.717	1.16
10	10	0.259	0.895	0.894	0.887	0.974
11	10	0.230	0.962	0.962	0.956	1.05
12	4	0.257	0.899	0.895	0.860	1.39
13	10	0.178	1.04	1.04	1.03	1.13
14	12	0.150	1.04	1.04	1.04	1.11

Table 2. Digitized and adjusted values of the strains associated with the stress–strain curve given by Stowell (1951) and associated secant moduli ($G_s = \sigma_{eff}/3S$)

σ_{eff} (GPa)	ε^*	ε	S	G_s/G
0	0	0	0	1.00
0.129	2.00×10^{-3}	1.82×10^{-3}	1.61×10^{-3}	1.00
0.207	3.21×10^{-3}	2.91×10^{-3}	2.60×10^{-3}	1.00
0.241	3.81×10^{-3}	3.46×10^{-3}	3.08×10^{-3}	0.981
0.276	4.53×10^{-3}	4.13×10^{-3}	3.70×10^{-3}	0.934
0.295	5.00×10^{-3}	4.58×10^{-3}	4.12×10^{-3}	0.897
0.310	5.74×10^{-3}	5.30×10^{-3}	4.82×10^{-3}	0.807
0.323	7.00×10^{-3}	6.54×10^{-3}	6.03×10^{-3}	0.671
0.345	10.0×10^{-3}	9.51×10^{-3}	8.97×10^{-3}	0.482
0.358	12.0×10^{-3}	11.5×10^{-3}	10.9×10^{-3}	0.412
0.367	14.0×10^{-3}	13.5×10^{-3}	12.9×10^{-3}	0.356

Table 2 lists a few points taken from the stress–strain curve given by Stowell (1951). Since the pre-buckling stress in this experiment is uniaxial, its value is equal to the von Mises effective stress σ_{eff}. For clarity, the axial strain measured in the experiment is denoted by ε^*. Figure 1a shows that the Young's modulus E^* associated with the experimental results is given by

$$E^* = 64.5\,\text{GPa}, \tag{13}$$

which is lower than the value E appropriate for aluminum. This suggests that the compliance of the experimental apparatus caused an error in the strain measurement. To correct for this error, it is assumed that the actual value ε of axial strain is a linear function of σ_{eff} given by

$$\varepsilon = \varepsilon^* - c\sigma_{eff}, \tag{14}$$

where the constant c is determined by requiring that the Young's modulus of the corrected elastic response be E so that

$$\varepsilon = \frac{\sigma_{eff}}{E}, \quad \varepsilon^* = \frac{\sigma_{eff}}{E^*}, \quad c = \frac{1}{E^*} - \frac{1}{E} = 1.42\times10^{-3}\,\text{GPa}^{-1}. \tag{15a,b,c}$$

Using this correction procedure, the values of ε in Table 2 are given and the adjusted stress–strain curve is plotted in Fig. 1b.

Next, with the help of the constitutive equation (1b) for pressure, the total strain ε may be written in the form

$$\boldsymbol{\varepsilon} = \tfrac{1}{3}(\boldsymbol{\varepsilon}\cdot\mathbf{I})\mathbf{I} + \boldsymbol{\varepsilon}' = -\frac{p}{3k}\mathbf{I} + \boldsymbol{\varepsilon}'. \tag{16}$$

Thus, for monotonic uniaxial stress: the pressure $p = (-\sigma_{eff}/3)$, and eqns (1b), (2a,b) and (3) can be used to show that

$$S = \varepsilon_{eff} = \varepsilon - \frac{\sigma_{eff}}{9k}. \tag{17}$$

Furthermore, for elastic response (with $\boldsymbol{\varepsilon}_p = 0$), eqns (1c), (2) and (3) can be used to show that

$$\sigma_{eff} = 3G\varepsilon_{eff} = 3GS. \tag{18}$$

From eqns (17) and (18), together with the bulk modulus k in eqn (12a), the values of S

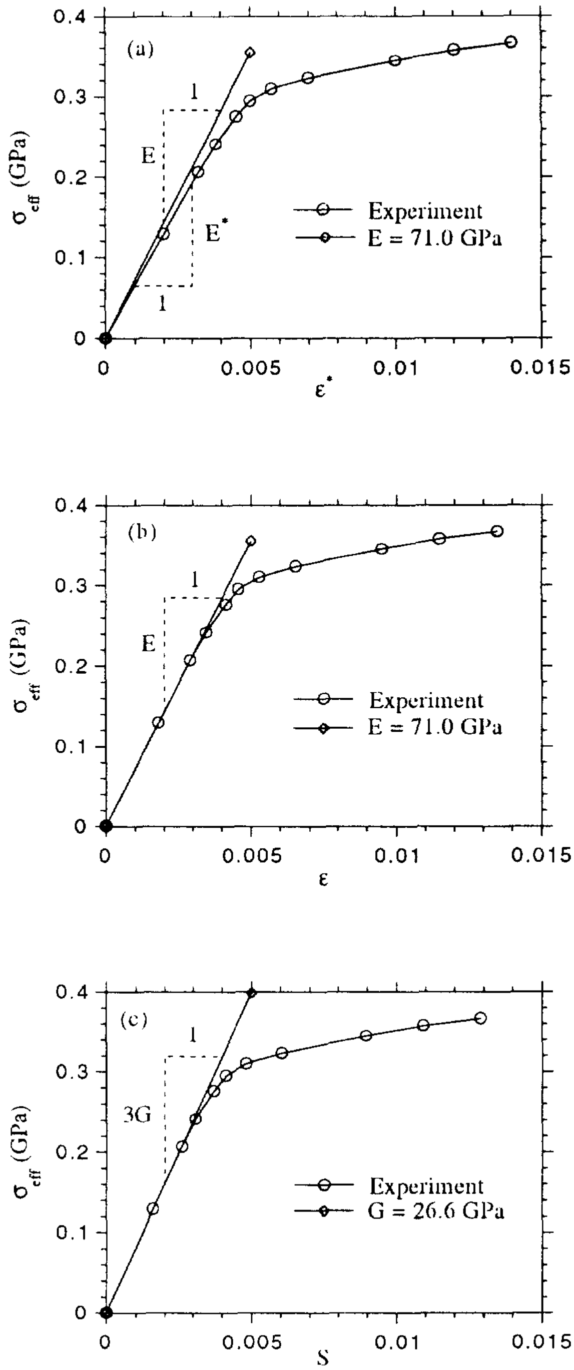

Fig. 1. (a) Original stress–strain curve of Stowell (1951); (b) adjusted stress–strain curve of Stowell (1951); (c) effective stress versus adjusted accumulated deviatoric total strain.

given in Table 2 are determined and σ_{eff} versus S is plotted in Fig. 1c. Also, the values of the secant shear modulus G_s associated with the adjusted experimental data defined by

$$G_s = \frac{\sigma_{eff}}{3S}, \tag{19}$$

are given in Table 2.

Table 3. Values of the normalized buckling stress from Gerard and Becker (1957)

σ^*_{cr} (GPa)	η
0.319	0.581
0.327	0.606
0.346	0.443
0.349	0.526
0.360	0.375
0.368	0.462
0.346	0.443
0.373	0.404

Figure 2 shows a plot of the normalized secant shear modulus together with the values of $\bar{G}/G$ determined by the buckling experiments of Stowell (1951) given in Table 1. The curve of G_s/G is piecewise linear because only those points given in Table 1 are plotted. For additional comparison, we have included values of η taken from the experimental data given by Gerard and Becker (1957) which are recorded in Table 3. These additional data points have been marked with a different symbol from those of Stowell (1951). It is noted that the curve of G_s/G in Fig. 2 is slightly different from the curve associated with the normalized secant extensional modulus E_s/E given by Gerard and Becker (1957: Fig. 5). These slight differences are caused by the fact that the values for G_s/G are obtained here using the adjusted experimental data of Stowell (1951) taking into account the finite value of the bulk modulus k (noting that $G_s/G = E_s/E$ only when k is infinite). Furthermore, the values of E_s/E plotted by Gerard and Becker (1957) were presumably taken from Table 2 of Gerard (1946), which were determined by his stress–strain curve (for the same material) and not the one given by Stowell (1951). In any case, results of the type presented in Fig. 2 have often been used to conclude that the normalized secant modulus provides a rather good prediction of the experimentally determined reduced shear modulus appropriate for inelastic buckling in torsion due to axial load.

Since shear stresses do not exist in the cruciform column prior to torsional buckling, the change in loading direction at the onset of buckling is similar to that associated with a 90° corner turning test. In fact, corner turning tests can, in principle, provide important experimental data on the reduced modulus and the non-coaxiality of plastic strain rate and deviatoric stress during non-proportional loading. Test results have been obtained by Ohashi and Ohno (1982) for corner turning conditions using axial force and internal pressure in thin-walled tubes of aluminum alloy 5056 at 200 C. In order to simplify the presentation of their experimental results which showed the influence of the third stress

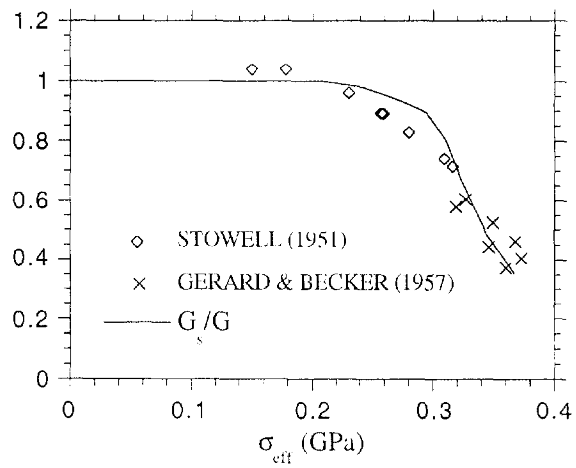

Fig. 2. Experimental values of $\bar{G}/G$ for Stowell (1951), η for Gerard and Becker (1957), and G_s/G for inelastic torsional buckling of a cruciform column.

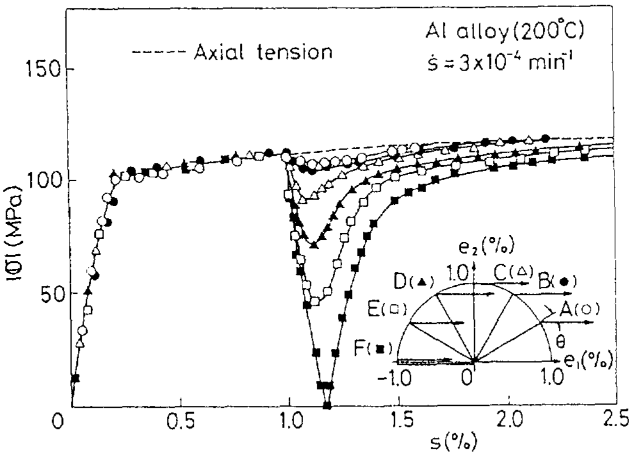

Fig. 3. Experimental results for corner turning tests presented in Fig. 9 of Ohashi and Ohno (1982).

invariant, Ohashi and Ohno (1982) defined a modified effective stress $\bar{\sigma}$ (see their eqn 14). However, results for the reduced modulus were not presented.

For our present purposes we define the direction of loading in the corner turning tests by specifying the components $\dot{\varepsilon}'_{ij}$ of the deviatoric total strain rate $\dot{\varepsilon}'$, relative to the fixed rectangular Cartesian base vectors $\mathbf{e}_i$ ($i = 1,2,3$), in terms of the expressions

$$\dot{\varepsilon}'_{11} = \dot{S}\cos\alpha, \quad \dot{\varepsilon}'_{22} = -\tfrac{1}{2}\dot{S}[\cos\alpha - \sqrt{3}\sin\alpha], \tag{20a,b}$$

$$\dot{\varepsilon}'_{33} = -\tfrac{1}{2}\dot{S}[\cos\alpha + \sqrt{3}\sin\alpha], \quad \text{all other } \dot{\varepsilon}'_{ij} = 0, \tag{20c,d}$$

where $\dot{S}$ is the accumulated strain rate defined by eqn (3) and the angle α determines the loading direction.

Figure 3 shows the results of corner turning tests [Ohashi and Ohno (1982: Fig. 9)] at an accumulated strain rate $\dot{S}$ of $5.0 \times 10^{-6}\ \mathrm{s}^{-1}$. For these tests, α takes one of the values [0°, 30°, 60°, 90°, 120°, 150°, 180°] for $0 \leqslant S < 0.01$ and then α is abruptly changed to the value of 0° for the remainder of the loading [$0.01 \leqslant S \leqslant 0.025$]. It is particularly noted that upon turning the corner the effective stress $\bar{\sigma}$ abruptly drops and then recovers to a value close to the value that was obtained in the proportional loading test. Also, with reference to Fig. 3, it is observed from the cyclic loading test ($\alpha = 180°$) that the Bauchinger effect is particularly strong during reverse loading.

3. B-P ELASTIC–VISCOPLASTIC MODEL

In this section, the constitutive equations for an elastic–viscoplastic metal which have evolved from the work of Bodner and Partom (1972, 1975) are reviewed. For convenience, this set of constitutive equations will be referred to as the B-P model.

Constitutive equations for the response of an elastic–viscoplastic metal have been developed by Bodner and Partom (1975) for isotropic hardening, and by Bodner (1985) for directional hardening (which models the Bauschinger effect). Since this theory is developed without the use of a yield surface or loading conditions, and since the effects of creep are incorporated in the plastic strain and hardening equations, the model has been referred to as a unified theory.

The unified theory reviewed by Bodner (1987) utilizes the Prandtl–Reuss flow rule of the form

$$\dot{\boldsymbol{\varepsilon}}_{\mathrm{p}} = \frac{\sqrt{3}\lambda}{\sigma_{\mathrm{eff}}}\boldsymbol{\sigma}', \tag{21}$$

where the scalar function λ is defined by

$$\lambda = D_0 \exp\left[-\frac{1}{2}\left(\frac{Z}{\sigma_{\mathrm{eff}}}\right)^{2n}\right]. \tag{22}$$

In eqn (22), D_0 and n are positive material constants, and Z is a measure of hardening which is separated additively into a scalar measure of isotropic hardening κ and a scalar measure $\boldsymbol{\beta}$ of directional hardening, such that

$$Z = \kappa + \beta. \tag{23}$$

The flow rule (21) is supplemented by evolution equations for κ and for a tensorial measure of directional hardening β, which in the absence of thermal recovery of hardening become

$$\dot{\kappa} = m_1 \dot{W}_{\mathrm{p}}(Z_1 - \kappa), \quad \dot{\boldsymbol{\beta}} = m_2 \dot{W}_{\mathrm{p}}(Z_3 \mathbf{U} - \boldsymbol{\beta}). \tag{24a,b}$$

In eqn (24), m_1 and m_2 are material constants that control the rate of hardening, $\dot{W}_{\mathrm{p}}$ is the usual expression for the rate of plastic work

$$\dot{W}_{\mathrm{p}} = \boldsymbol{\sigma}' \cdot \dot{\boldsymbol{\varepsilon}}_{\mathrm{p}}, \tag{25}$$

and Z_1 and Z_3 are material constants which control the saturated values of κ and β, respectively. Furthermore, the unit tensor $\mathbf{U}$ and the scalar measure of directional hardening β are specified by

$$\mathbf{U} = \frac{\boldsymbol{\sigma}}{|\boldsymbol{\sigma}|}, \quad \beta = \boldsymbol{\beta} \cdot \mathbf{U}. \tag{26a,b}$$

More recent work of Rubin (1987a, 1989) considered elastic–viscoplastic constitutive equations for large deformations which exhibit a continuity of solid and fluid states. For the small deformation version of these equations, the flow rule (21) and the expression for $\mathbf{U}$ in eqn (26a) take the modified forms

$$\dot{\boldsymbol{\varepsilon}}_{\mathrm{p}} = \Gamma \mathbf{A}, \quad \mathbf{A} = \frac{\boldsymbol{\sigma}'}{2G}, \tag{27a,b}$$

$$\mathbf{U} = \frac{\boldsymbol{\sigma}'}{|\boldsymbol{\sigma}'|}, \tag{27c}$$

where Γ is a scalar function of the form

$$\Gamma = \Gamma_0 \exp\left[-\frac{1}{2}\left(\frac{Z}{\sigma_{\mathrm{eff}}}\right)^{2n}\right], \tag{28}$$

and Γ_0 is a positive material constant. It is noted from eqns (27a) and (28) that for large values of plastic strain rate (or large values of stress $\sigma_{\mathrm{eff}} \gg Z$) the flow rule (27a,b) yields a fluid-like response because the plastic strain rate increases linearly with stress

$$\dot{\varepsilon}_p \approx \frac{\Gamma_0}{2G}\boldsymbol{\sigma}'. \tag{29}$$

In contrast, the flow rule (21) with the specification (22) predicts that, in the same limit, the magnitude of plastic strain rate is bounded

$$|\dot{\boldsymbol{\varepsilon}}_p|_{max} \approx \sqrt{2D_0}. \tag{30}$$

In spite of this difference it can be shown (Rubin, 1990) that for small and moderate values of plastic strain rate, the exponential function in eqns (22) and (28) dominates, and the responses predicted by eqns (21) and (27a) are nearly the same when Γ_0 is determined by the values of D_0, the shear modulus G, and a representative value of flow stress $\sigma_{eff} \approx Y$, such that

$$\Gamma_0 = \left(\frac{2\sqrt{3}G}{Y}\right)D_0. \tag{31}$$

In the present paper, the modified flow rule (27) with the specification (28) is used instead of (21), but similar results would be obtained with the original equations. For both forms, the parameter n mainly controls the rate-sensitivity of the response, with high rate-sensitivity for small values of n and low rate-sensitivity for large values of n. Thus, the response becomes nearly rate-independent when n becomes very large.

The direction $\mathbf{U}$ was modified by Rubin (1987b) to take the form (27c) in terms of the deviatoric stress $\boldsymbol{\sigma}'$ instead of (26a) in terms of the total stress $\boldsymbol{\sigma}$ in order to retain the influence of directional hardening in high pressure applications. Nevertheless, the use of the total stress to define the direction $\mathbf{U}$ has proven to be useful for a number of applications in which the pressure did not become too large.

4. MODIFICATION OF THE FLOW RULE

For general non-proportional loading paths it is possible to quantify the notion of the reduced effective shear modulus by defining the reduction factor R such that

$$R = \frac{\dot{\boldsymbol{\sigma}}'}{2G|\dot{\boldsymbol{\varepsilon}}'|}\cdot\frac{\dot{\boldsymbol{\varepsilon}}'}{|\dot{\boldsymbol{\varepsilon}}'|} = \left[1-\frac{\dot{\boldsymbol{\varepsilon}}_p}{|\dot{\boldsymbol{\varepsilon}}'|}\cdot\frac{\dot{\boldsymbol{\varepsilon}}'}{|\dot{\boldsymbol{\varepsilon}}'|}\right] \quad \text{for } \dot{\boldsymbol{\varepsilon}}' \neq 0. \tag{32}$$

In a more general setting Hashiguchi (1993) used expressions somewhat similar to eqn (32) to define stiffness moduli. Here, the value of R quantifies the amount by which the shear modulus is instantaneously reduced because it determines the component of the deviatoric stress rate in the direction of the loading, divided by $2G$ times the magnitude of the strain rate. Notice that the value of R depends on both the magnitude and the direction of the deviatoric total strain rate $\dot{\boldsymbol{\varepsilon}}'$ and plastic strain rate $\dot{\boldsymbol{\varepsilon}}_p$.

Motivated by this observation, a modified theory is developed in this section which specifically changes the flow rule (27a) so that the plastic strain rate can be non-coaxial with the deviatoric stress. This modification also causes the incremental elastic–viscoplastic theory to indicate a reduced effective shear modulus in corner turning tests. Modifications causing the drop in effective stress observed in the tests shown in Fig. 3 will be discussed in the next section.

Firstly, in order to model the non-coaxiality of the plastic strain rate and the deviatoric stress, the flow rule (27a) is modified to take the form

$$\dot{\varepsilon}_p = \Gamma \mathbf{A} + g(\Gamma) f \mathbf{N}, \tag{33}$$

where $\mathbf{A}$ is specified by (27b), Γ is specified by (28), and $\mathbf{N}$ is a deviatoric tensor which is perpendicular to the deviatoric stress

$$\mathbf{N} \cdot \mathbf{I} = 0, \quad \mathbf{N} \cdot \boldsymbol{\sigma}' = 0. \tag{34a,b}$$

The non-negative function $g(\Gamma)$ and the parameter f are described later.

In order to model the reduced effective shear modulus observed in corner tests, it is essential in the present formulation to assume that plastic strain rate is an explicit function of total strain rate. Specifically, $\mathbf{N}$ is taken to be the component of the deviatoric total strain rate $\dot{\boldsymbol{\varepsilon}}'$ which is normal to the deviatoric stress $\boldsymbol{\sigma}'$ such that

$$\mathbf{N} = \dot{\boldsymbol{\varepsilon}}' - (\dot{\boldsymbol{\varepsilon}}' \cdot \mathbf{B})\mathbf{B}, \tag{35}$$

where $\mathbf{B}$ is the direction of deviatoric stress defined by

$$\mathbf{B} = \frac{\boldsymbol{\sigma}'}{|\boldsymbol{\sigma}'|}. \tag{36}$$

It is important to note that since $\mathbf{N}$ depends explicitly on $\dot{\boldsymbol{\varepsilon}}'$, it is immediately sensitive to changes in the direction of deviatoric strain rate which are characteristic of a corner test.

In contrast to most constitutive equations for viscoplasticity, it is assumed here that the plastic strain rate can depend on the total strain rate. Such a generalization allows for the possibility of a term like $\mathbf{N}$ in the flow rule (33). From a physical viewpoint, this means that under multiaxial, non-proportional loadings the mobile dislocation density and/or the velocity of mobile dislocations would depend on the deviatoric total strain rate, in magnitude and direction, in addition to the stress and hardening properties, which is reasonable.

It is interesting to note that various investigators have examined the case, somewhat related to eqn (33), of plastic straining due to a stress rate component tangential to a yield surface. A formulation of this kind and a review of earlier work was presented recently by Hashiguchi (1993).

Returning to the form (33) of the flow rule, it is noted that for proportional loading, the evolution of plasticity causes the deviatoric stress $\boldsymbol{\sigma}'$ to align with the direction of deviatoric total strain rate $\dot{\boldsymbol{\varepsilon}}'$, which causes $\mathbf{N}$ to vanish so that the form (33) reduces to (27a,b). However, for non-proportional loading $\mathbf{N}$ does not vanish and plastic strain rate has a component normal to deviatoric stress. This deviation from proportional loading can be quantified by defining the phase angles $\theta(\dot{\boldsymbol{\varepsilon}}')$ and $\theta(\dot{\boldsymbol{\varepsilon}}_p)$ relative to the direction of deviatoric stress $\mathbf{B}$ by

$$\theta(\dot{\boldsymbol{\varepsilon}}') = \cos^{-1}\left[\frac{\dot{\boldsymbol{\varepsilon}}'}{|\dot{\boldsymbol{\varepsilon}}'|} \cdot \mathbf{B}\right], \quad \theta(\dot{\boldsymbol{\varepsilon}}_p) = \cos^{-1}\left[\frac{\dot{\boldsymbol{\varepsilon}}_p}{|\dot{\boldsymbol{\varepsilon}}_p|} \cdot \mathbf{B}\right], \tag{37a,b}$$

such that $\theta(\dot{\boldsymbol{\varepsilon}}')$ and $\theta(\dot{\boldsymbol{\varepsilon}}_p)$ are in the range $[0,\pi]$ and vanish for proportional loading. It will be shown in the corner tests simulated later in this section that when the corner is turned, $\theta(\dot{\boldsymbol{\varepsilon}}')$ and $\theta(\dot{\boldsymbol{\varepsilon}}_p)$ experience abrupt increases to values less than $\pi/2$. Then for subsequent maintained proportional loading following the corner turn, the values of $\theta(\dot{\boldsymbol{\varepsilon}}')$ and $\theta(\dot{\boldsymbol{\varepsilon}}_p)$ decay back to zero.

Next, it can be shown that the flow rule (33) also models the reduced effective modulus in shear observed in a corner test. To this end, use is made of eqns (1), (27), (33) and (36) to obtain the expressions

$$\dot{\boldsymbol{\sigma}} = k(\mathbf{I} \cdot \dot{\boldsymbol{\varepsilon}})\mathbf{I} + \dot{\boldsymbol{\sigma}}', \tag{38a}$$

$$\dot{\boldsymbol{\sigma}}' = 2G\dot{\boldsymbol{\varepsilon}}' - 2Gg(\Gamma) f \mathbf{N} - \Gamma|\boldsymbol{\sigma}'|\mathbf{B}. \tag{38b}$$

Moreover, with the help of the definition (35) the component $\dot{\sigma}_{ij}$ of the stress rate can be written in the form

$$\dot{\sigma}_{ij} = L_{ijkl}\dot{\varepsilon}_{kl} - \Gamma\sigma'_{ij}, \quad L_{ijkl} = L^{\mathrm{E}}_{ijkl} + L^{\mathrm{VP}}_{ijkl}, \tag{39a,b}$$

$$L^{\mathrm{E}}_{ijkl} = k\delta_{ij}\delta_{kl} + 2GH_{ijkl}, \quad L^{\mathrm{VP}}_{ijkl} = -2Gg(\Gamma)f[H_{ijkl} - B_{ij}B_{kl}], \tag{39c,d}$$

$$H_{ijkl} = [\tfrac{1}{2}(\delta_{ik}\delta_{jl} + \delta_{il}\delta_{jk}) - \tfrac{1}{3}\delta_{ij}\delta_{kl}], \tag{39e}$$

where $\dot{\varepsilon}_{ij}$, σ'_{ij} and B_{ij} are the components of $\dot{\boldsymbol{\varepsilon}}$, $\boldsymbol{\sigma}'$, and $\mathbf{B}$, respectively, δ_{ij} are the components of the Kronecker delta and H_{ijkl} is a fourth order tensor which operates on a second order tensor to obtain its deviatoric symmetric part. The fourth order tensor L_{ijkl} is separated into an elastic part L^{E}_{ijkl} and a viscoplastic part L^{VP}_{ijkl} to emphasize that the present model is not contained in the class of constitutive equations analysed by Tvergaard (1988) which does not include a term like L^{VP}_{ijkl}.

Now, eqn (37a) can be used to rewrite expression (32) for the reduction factor R in the form

$$R = \left[1 - \frac{\Gamma|\boldsymbol{\sigma}'|}{2G|\dot{\boldsymbol{\varepsilon}}'|}\cos\theta(\dot{\boldsymbol{\varepsilon}}') - g(\Gamma)f\{1 - \cos^2\theta(\dot{\boldsymbol{\varepsilon}}')\}\right] \quad \text{for } \dot{\boldsymbol{\varepsilon}}' \neq 0. \tag{40}$$

This expression shows the explicit dependence of R on the angle $\theta(\dot{\boldsymbol{\varepsilon}}')$ between the deviatoric stress and the deviatoric strain rate. For the case of proportional loading $\theta(\dot{\boldsymbol{\varepsilon}}')$ vanishes and eqns (32) and (40) yield the result that

$$R = \left[1 - \frac{|\dot{\boldsymbol{\varepsilon}}_{\mathrm{p}}|}{|\dot{\boldsymbol{\varepsilon}}'|}\right] = \left[1 - \frac{\Gamma|\boldsymbol{\sigma}'|}{2G|\dot{\boldsymbol{\varepsilon}}'|}\right] \quad \text{for } \dot{\boldsymbol{\varepsilon}}' \neq 0. \tag{41}$$

For monotonic proportional loading, the tensors $\boldsymbol{\sigma}'$, $\boldsymbol{\varepsilon}'$, $\boldsymbol{\varepsilon}_{\mathrm{p}}$ and their rates have the same constant direction so that eqn (2a,b) can be used together with the definition (32) to deduce that

$$R = \frac{\dot{\sigma}_{\mathrm{eff}}}{3G\dot{\varepsilon}_{\mathrm{eff}}} = \frac{G_{\mathrm{t}}}{G}, \tag{42}$$

which can be recognized as the normalized tangent modulus in shear G_{t}. Furthermore, using expression (17) and the standard definition of the tangent extensional modulus E_{t},

$$E_{\mathrm{t}} = \frac{\dot{\sigma}_{\mathrm{eff}}}{\dot{\varepsilon}}, \tag{43}$$

where $\dot{\varepsilon}$ is the axial strain rate and $\sigma_{\mathrm{eff}} = \sigma$ in a uniaxial stress test, it can be shown that a relationship of the type (6a) holds with $\bar{E}$ and $\bar{G}$ replaced by E_{t} and G_{t}. Consequently, for monotonic proportional loading the reduction factor R can be expressed as a function of E_{t} and elastic constants. Further in this regard, it is noted that the approximation discussed by Bodner *et al.* (1991) and Bodner (1992) for that case allows R to be expressed as a function of the stress and hardening variables only.

Alternatively, if the corner is turned abruptly, $\theta(\dot{\boldsymbol{\varepsilon}}')$ instantaneously becomes $\pi/2$ and eqn (40) reduces to

$$R = 1 - g(\Gamma)f \quad \text{for } \dot{\boldsymbol{\varepsilon}}' \neq 0, \tag{44}$$

which can be seen to be independent of the magnitude of the total strain rate. As another limiting case, the direction of the deviatoric total strain rate can be kept constant and its magnitude can be increased abruptly. Since Γ and $\boldsymbol{\sigma}'$ are explicitly independent of total strain rate, when the magnitude of the total strain rate becomes large, expression (40) reduces to

$$R = [1-g(\Gamma)f\{1-\cos^2\theta(\dot{\varepsilon}')\}] \quad \text{for } \dot{\varepsilon}' \neq 0. \tag{45}$$

This shows that the response to an abrupt change in total strain rate becomes elastic if the loading is proportional [with $\theta(\dot{\varepsilon}') = 0$] and smoothly transitions to the limiting value (44) as $\theta(\dot{\varepsilon}')$ approaches $\pi/2$.

Returning to the result (44) it is noted that the value of the reduction factor R is independent of the value of $|\dot{\varepsilon}'|$, and is controlled by the value of $g(\Gamma)f$. Physical considerations require R to remain in the range zero to unity. Thus, constitutive equations must be specified which require

$$0 \leqslant g(\Gamma)f \leqslant 1. \tag{46}$$

For definiteness, it is assumed that $g(\Gamma)$ is a non-decreasing function which satisfies the properties that

$$g(0) = 0, \quad g(\infty) = 1, \quad \frac{dg}{d\Gamma} \geqslant 0. \tag{47a,b,c}$$

The condition (47a) is imposed to ensure that the reduction factor R in (44) will remain unity whenever plastic deformation vanishes ($\Gamma = 0$). Also, condition (47b) is imposed so that the restriction (46) will require the simple condition that the value of the parameter f remains less than unity. The specific functional form for $g(\Gamma)$ should be motivated by experimental data which are presently unavailable. However, for the simulations presented later, the simple form

$$g(\Gamma) = \frac{\Gamma}{b+\Gamma} \tag{48}$$

is specified which has the desired features (47) and is controlled by a single material constant b. For simplicity, the value of b will be taken sufficiently small so that $g(\Gamma)$ essentially becomes the Heavyside function which is equal to unity during plastic deformation with positive Γ.

Now, with the help of eqns (44) and (48) it can be shown that the factor $(1-f)$ controls the minimum value of the reduced effective shear modulus since

$$R = [1-g(\Gamma)f] \geqslant (1-f). \tag{49}$$

In order to motivate a functional form for the parameter f, it is noted that from a physical point of view f is expected to depend on the hardening parameters. Since directional hardening usually increases much more rapidly than isotropic hardening (Chan *et al.*, 1988), the stress–strain curve shown in Fig. 1c suggests that directional hardening is increasing rapidly in the range $\{0.22 \text{ GPa} \leqslant \sigma_{\text{eff}} \leqslant 0.32 \text{ GPa}\}$ after which isotropic hardening continues to harden. Using the result (44) to interpret the torsional buckling experiments shown in Fig. 2, one concludes that the value of f starts out at zero and increases in a bilinear manner with both directional and isotropic hardening variables. This basic character can be represented in terms of the hardening variables and related constants,

$$f = f_1\left[\frac{|\boldsymbol{\beta}|}{Z_3}\right]+f_2\left[\frac{\kappa-\kappa_0}{Z_1-\kappa_0}\right], \quad f_1+f_2 < 1, \tag{50a,b}$$

where f_1 and f_2 are material constants, and κ_0 is the initial value of κ. Also, the condition (50b) is imposed in order to satisfy the restriction (46). Further in this regard, it is noted that for proportional monotonic loading the value of $|\boldsymbol{\beta}|$ approaches Z_3 and κ approaches Z_1 so that f approaches its saturated value of (f_1+f_2). This means that the minimum value of the reduction factor R is $(1-f_1-f_2)$, which remains positive and ensures that there is always some resistance to torsional inelastic buckling. In contrast, the secant modulus associated with eqn (19) predicts the unphysical result that the reduction factor G_s/G approaches zero for continued monotonic loading.

In summary, it is noted that aside from the standard equations for stress (1) and effective stress (2), the modified theory of this section is characterized by: the modified flow rule (33) for plastic strain rate with **A** given by (27b), Γ given by (28), **N** given by (35), and $g(\Gamma)$ given by (48); the expression (23) for the scalar measure of hardening Z, evolution equations for hardening (24a,b) with the modified direction **U** given by (27c) and expression (26b) for the scalar measure of directional hardening β; and the equation (50a) for the function f which controls the value of the reduced effective shear modulus in corner turning tests. These differential equations (33), (24a), and (24b) are integrated, subject to the initial conditions

$$\boldsymbol{\varepsilon}_p(0) = \boldsymbol{\varepsilon}_{p0}, \quad \kappa(0) = \kappa_0, \quad \boldsymbol{\beta}(0) = \boldsymbol{\beta}_0. \tag{51a,b,c}$$

For the examples considered in this section and the next, it is assumed that the material is stress-free and fully isotropic in the initial configuration so that

$$\boldsymbol{\varepsilon}_{p0} = 0, \quad \boldsymbol{\beta}_0 = 0. \tag{52a,b}$$

In addition to the material constants $\{\Gamma_0, n, Z_1, Z_3, m_1, m_2\}$ associated with the B-P theory of Section 3, the modified theory of this section requires only three material constants $\{b, f_1, f_2\}$ in eqns (48) and (50a), which characterize the response to corner turning tests. For the modifications introduced in this section, the restriction imposed by the second law of thermodynamics [e.g. Rubin (1989)] which requires plastic deformation to be dissipative with the rate of plastic work $\dot{W}_p$ being non-negative,

$$\dot{W}_p = \boldsymbol{\sigma}' \cdot \dot{\boldsymbol{\varepsilon}}_p = \frac{\Gamma \sigma_{\text{eff}}^2}{3G} \geqslant 0, \tag{53}$$

is satisfied automatically since Γ is non-negative.

To exhibit the predictions of the modified theory of this section, attention was confined to isochoric deformation ($\boldsymbol{\varepsilon} = \boldsymbol{\varepsilon}'$) with the components of $\boldsymbol{\varepsilon}'$ given by eqn (20). Then, values of the material constants appropriate for matching the experimental stress–strain curve of Stowell (1951) in the form of Fig. 1c and the test results shown in Fig. 2 were determined:

$$G = 26.6\,\text{GPa}, \tag{54a}$$

$$\Gamma_0 = 10^8\,\text{s}^{-1}, \quad n = 5, \tag{54b,c}$$

$$m_1 = 290\,\text{GPa}^{-1}, \quad \kappa_0 = 0.33\,\text{GPa}, \quad Z_1 = 0.50\,\text{GPa}, \tag{54d,e,f}$$

$$m_2 = 20{,}000\,\text{GPa}^{-1}, \quad Z_3 = 0.12\,\text{GPa}, \tag{54g,h}$$

$$b = 10^{-6}\,\text{s}^{-1}, \quad f_1 = 0.23, \quad f_2 = 0.70. \tag{54i,j,k}$$

The value of G is the same as in eqn (12c); the value of Γ_0 is representative of 6061-T6 aluminum (Rubin, 1990); the value of n is representative of aluminum at room temperature (Bodner, 1987); and the value of b was chosen to be about three orders of magnitude lower than the value of Γ during loading. This small value of b was chosen so that $g(\Gamma)$ is nearly the Heavyside function which vanishes when Γ vanishes and equals unity when Γ is positive. The values of $\{m_1, \kappa_0, Z_1, m_2, Z_3\}$ were chosen to produce reasonably close correspondence

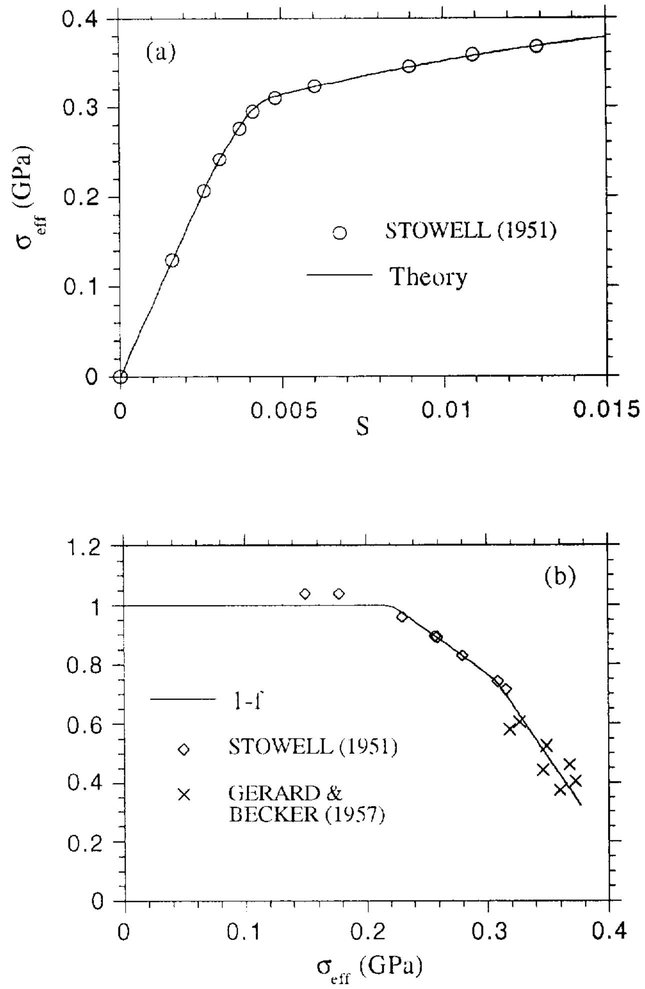

Fig. 4. (a) Comparison of the simulated stress strain curve with points from the experimental curve of Stowell (1951); (b) theoretical predictions of the reduced modulus $(1-f)$ compared with experimental values of $\bar{G}/G$ for Stowell (1951), and η for Gerard and Becker (1957).

with the monotonic loading experimental stress–strain curve (see Fig. 4a) with $\dot{S} = 5.0 \times 10^{-6}\,s^{-1}$, and the constants $\{f_1, f_2\}$ were chosen to produce reasonable values for the reduced effective modulus in shear. In particular, Fig. 4b shows the experimental results of Stowell (1948) and of Gerard and Becker (1957) together with the value of $R \approx (1-f)$. It seems that the proposed expression for f yields reasonably good values of the reduced effective shear modulus for inelastic bucking of the cruciform column.

The response to corner turning tests of the type performed by Ohashi and Ohno (1982) was also considered, again with $\dot{S} = 5.0 \times 10^{-6}\,s^{-1}$. To model their aluminum alloy, the following material constants were specified:

$$G = 26.6\,\text{GPa}, \tag{55a}$$

$$\Gamma_0 = 10^8\,s^{-1}, \quad n = 1, \tag{55b,c}$$

$$m_1 = 1{,}000\,\text{GPa}^{-1}, \quad \kappa_0 = 0.4\,\text{GPa}, \quad Z_1 = 0.53\,\text{GPa}, \tag{55d,e,f}$$

$$m_2 = 40{,}000\,\text{GPa}^{-1}, \quad Z_3 = 0.3\,\text{GPa}, \tag{55g,h}$$

$$b = 10^{-6}\,s^{-1}, \quad f_1 = 0.23, \quad f_2 = 0.70. \tag{55i,j,k}$$

The values of $\{G, \Gamma_0, b, f_1, f_2\}$ were not changed, but the values of $\{m_1, \kappa_0, Z_1, m_2, Z_3\}$ were chosen to approximately match the response to monotonic proportional loading with

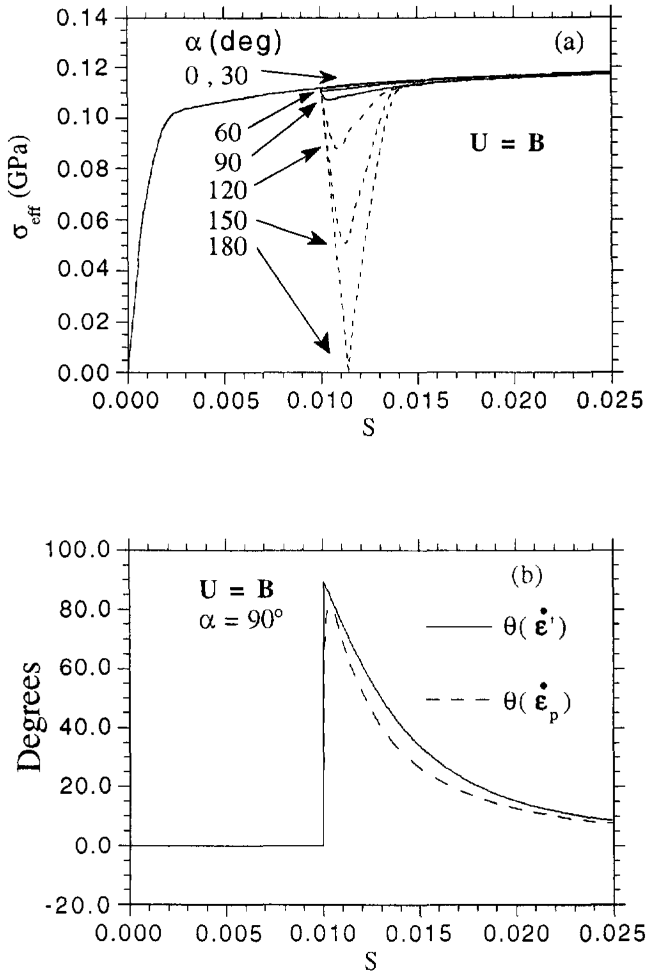

Fig. 5. Predictions using the theory of Section 4. (a) Simulations of corner turning tests; (b) non-coaxiality of deviatoric total and plastic strain rates relative to the direction of deviatoric stress.

$\alpha = 0$ in eqn (20) (it is noted that their modified definition of effective stress $\bar{\sigma}$ is not equal to σ_{eff}). Also, the value of n was chosen to be representative of aluminum at elevated temperature (Bodner, 1987). Figure 5a shows the response to simulations with α taking one of the values [0°, 30°, 60°, 90°, 120°, 150°, 180°] for $0 \leqslant S < 0.01$ and then abruptly changing to the value of 0° for the remainder of the loading [$0.01 \leqslant S \leqslant 0.025$]. The curves for $\alpha = 120°$, 150°, and 180° are shown as broken lines because the strong Bauschinger effect exhibited by the experiments (Fig. 3) is not modeled well by the simulation. On this matter, the hardening constants (55d–h) were chosen to obtain good fitting of the initial portion of the monotonic curve without regard to the fully reversed loading curve. Figure 5b exhibits the non-coaxiality of plastic strain rate by showing the angles $\theta(\dot{\varepsilon}')$ and $\theta(\dot{\varepsilon}_p)$ defined by eqn (37a,b) and predicted for a corner turning test with $\alpha = 90°$ for $0 \leqslant S < 0.01$. In Fig. 5b, turning the corner leads to abrupt increases of the angles $\theta(\dot{\varepsilon}')$ and $\theta(\dot{\varepsilon}_p)$ to near 90°, followed by slow decreases toward zero.

Comparison of the experimental results shown in Fig. 3 with predictions of Fig. 5a indicates that the drops in effective stress for the tests with $\alpha \neq \{180° \text{ or } 0°\}$ are smaller than those observed in the experiments. Consequently, an additional modification of the theory is developed in the next section which enhances the magnitudes of these drops.

5. MODIFICATIONS OF DIRECTIONAL HARDENING

The differences between the experimental results shown in Fig. 3 and the predictions shown in Fig. 5a indicate that the effective stress drops more rapidly and drops to a lower value in the experiments. Such a large drop appears to be consistent with a physical interpretation that a change in straining direction activates new slip planes which are initially unhardened. Consequently, this change will primarily influence directional hardening. In order to properly model this effect, two modifications of the scalar measure β of directional hardening are proposed.

Firstly, it is assumed that the direction **U** in the evolution equation (24b) is different from the direction **B** of deviatoric stress (36) used to define the scalar measure β of directional hardening (26b). Specifically, **U** is specified by the direction of plastic strain rate and β is the component of $\boldsymbol{\beta}$ in the direction of deviatoric stress, as previously, so that

$$\mathbf{U} = \frac{\dot{\boldsymbol{\varepsilon}}_p}{|\dot{\boldsymbol{\varepsilon}}_p|}, \quad \beta = \boldsymbol{\beta} \cdot \mathbf{B}. \tag{56a,b}$$

Secondly, it is assumed that the constant m_2 in eqn (24b), which controls the rate of directional hardening, is a function of the direction of deviatoric strain rate of the form

$$m_2 = m_{20} \exp\left[a_2 \sin \theta(\dot{\varepsilon}')\right], \tag{57}$$

where m_{20} and a_2 are material constants and $\theta(\dot{\boldsymbol{\varepsilon}}')$ is defined by eqn (37a). This causes the rate m_2 to increase for non-proportional loadings.

The influence of these modifications can be explained by considering a 90° corner turning test in which the direction of the deviatoric total strain rate is abruptly changed. During proportional loading into the plastic range, the directional hardening tensor $\boldsymbol{\beta}$ evolves in the direction **U** of plastic strain rate such that the scalar β tends to saturate at the value Z_3. Under these conditions the directions **U** and **B** coincide, the normal tensor **N** vanishes and $m_2 = m_{20}$, so the theory reduces to that discussed at the end of the last section. However, in response to an abrupt change in the direction of total strain rate, the plastic strain rate instantaneously obtains a component parallel to $\mathbf{N}(\mathbf{N} \cdot \mathbf{B} = 0)$, so that $\boldsymbol{\beta}$ tends to evolve in a direction different from **B**. This causes a decrease in the value of the scalar β which, in turn, causes a decrease in the value of effective stress σ_{eff}. Also, the value of m_2 is increased at the instant of direction change to the value $m_{20} \exp(a_2)$, which causes the drop in β to develop more rapidly.

Additional simulations of the corner turning tests were performed with this modified theory using the material constants (55), except that m_2 in (55g) is replaced by the function (57) with

$$m_{20} = 40{,}000\,\text{GPa}^{-1}, \quad a_2 = 3, \tag{58a,b}$$

which is the value of m_2 given previously by (55g). Figure 6 shows the influence of these

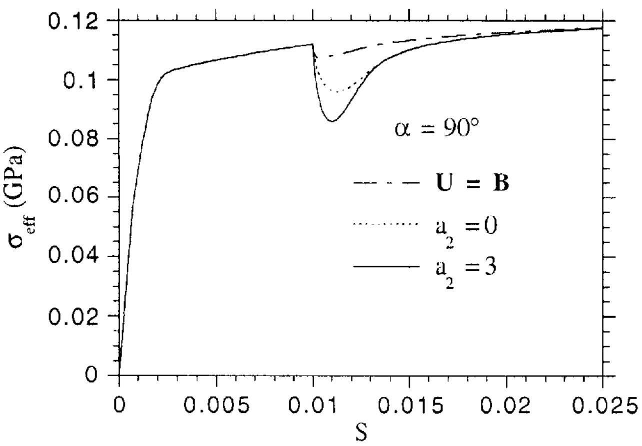

Fig. 6. Comparison of simulations of a 90° corner turning test using the theory of Section 4 (**U** = **B**) with those using the theory of Section 5 (a_2 = 0 and 3).

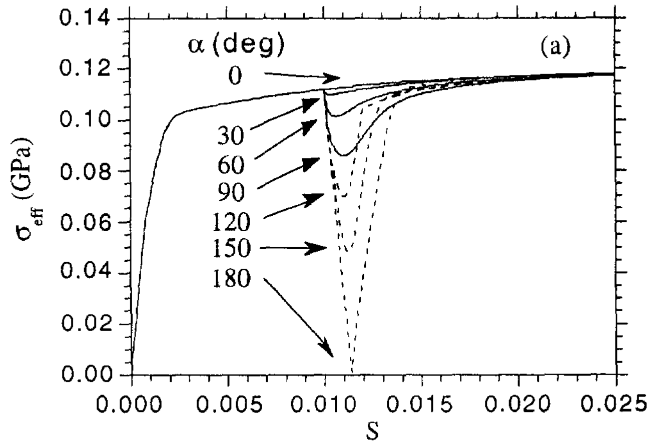

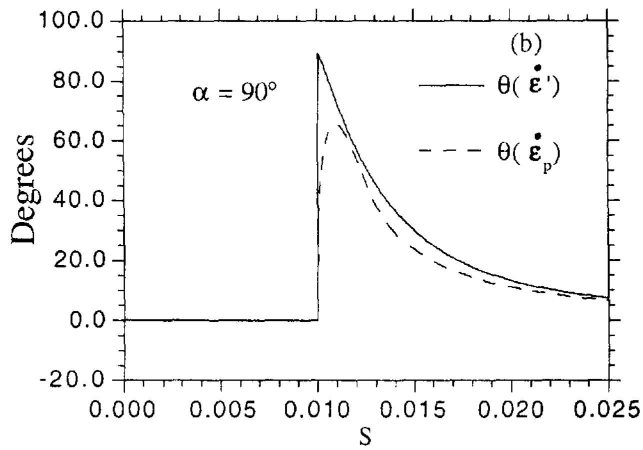

Fig. 7. Predictions using the theory of Section 5. (a) Simulations of corner turning tests; (b) non-coaxiality of deviatoric total and plastic strain rates relative to the direction of deviatoric stress.

modifications for the 90° corner turning case, and Fig. 7a shows that the overall predictions of the modified theory of this section are much closer to the experimental data in Fig. 3. However, the strong Bauschinger effect indicated by the experimental data is still not adequately modeled by the modified theory. Finally, Fig. 7b shows the non-coaxiality for a 90° corner turning test.

6. A SIMPLE RATE-INDEPENDENT THEORY

In order to emphasize the importance of the rate-dependent nature of the viscoplastic theory developed here, it is useful to discuss some of the difficulties encountered in attempting to develop an associated rate-independent theory that would indicate the same effects as the modified model of Sections 4 and 5. To this end, it is noted that the viscoplastic model of Sections 4 and 5 predicts a relatively rate-insensitive response when the parameter n in (28) becomes very large. This is because, for large values of n, the function Γ in (28) nearly vanishes whenever σ_{eff} is less than the hardening parameter Z. Thus it is natural to consider an associated rate-independent theory which uses a yield function F of the form

$$F = F(\boldsymbol{\varepsilon}, \boldsymbol{\varepsilon}_p, \kappa, \boldsymbol{\beta}) = \frac{\sigma_{eff}}{Z} - 1, \tag{59}$$

where $\boldsymbol{\varepsilon}_p, \kappa, \boldsymbol{\beta}$ are determined by the evolution equations (33),(24a) and (24b), respectively.

Moreover, for rate-independent response the function $g(\Gamma)$ in the modified flow rule (33) is specified to be the Heavyside function

$$g(\Gamma) = H(\Gamma) = \begin{cases} 0 & \text{for} \quad \Gamma \leqslant 0 \\ 1 & \text{for} \quad \Gamma > 0. \end{cases} \tag{60a}$$

Within this context, the value of Γ is no longer determined by the functional form (28) but rather is determined by a consistency condition which requires $\dot{F}$ to vanish during plastic loading.

At present it does not seem possible to prove that the resulting value of Γ is positive for all loading situations. Moreover, in view of the condition (53), this indicates that plastic deformation may not always be dissipative so that the second law of thermodynamics may not be satisfied. However, for the simpler case when directional hardening is neglected ($\boldsymbol{\beta} = 0$), with

$$F = F(\boldsymbol{\varepsilon}, \boldsymbol{\varepsilon}_{\mathrm{p}}, \kappa) = \frac{\sigma_{\mathrm{eff}}}{\kappa} - 1, \tag{60b}$$

it can be shown using the consistency condition associated with loading conditions in strain space (Naghdi and Trapp, 1975) that Γ is given by

$$\Gamma = 0 \quad \text{for} \quad \{F < 0\} \text{ or } \{F = 0 \text{ and } \boldsymbol{\sigma}' \cdot \dot{\boldsymbol{\varepsilon}}' \leqslant 0\}, \tag{61a}$$

$$\Gamma = \frac{9G^2 \boldsymbol{\sigma}' \cdot \dot{\boldsymbol{\varepsilon}}'}{\kappa^2[3G + \kappa m_1(Z_1 - \kappa)]} \quad \text{for} \quad \{F = 0 \text{ and } \boldsymbol{\sigma}' \cdot \dot{\boldsymbol{\varepsilon}}' > 0\}. \tag{61b}$$

It is noted that since Γ in eqn (61b) is positive during loading, the plastic dissipation given by (53) is also positive.

With the help of eqns (38), (40), (60) and (61) it can be shown that during elastic response, unloading, or neutral loading

$$\dot{\boldsymbol{\sigma}}' = 2G(\mathbf{B} \cdot \dot{\boldsymbol{\varepsilon}}')\mathbf{B} + 2G\mathbf{N}, \quad R = 1, \tag{62a,b}$$

whereas during loading

$$\dot{\boldsymbol{\sigma}}' = 2G\left[1 - \frac{3G}{[3G + \kappa m_1(Z_1 - \kappa)]}\right](\mathbf{B} \cdot \dot{\boldsymbol{\varepsilon}}')\mathbf{B} + 2G[1 - f]\mathbf{N}, \tag{63a}$$

$$R = \left[1 - \frac{3G\cos^2\theta(\dot{\boldsymbol{\varepsilon}}')}{[3G + \kappa m_1(Z_1 - \kappa)]} - f\{1 - \cos^2\theta(\dot{\boldsymbol{\varepsilon}}')\}\right] \quad \text{for } \dot{\boldsymbol{\varepsilon}}' \neq 0. \tag{63b}$$

It then follows from eqns (61) and (62) that for a 90° corner turning test $\boldsymbol{\sigma}' \cdot \dot{\boldsymbol{\varepsilon}}'$ vanishes and the response corresponds to neutral loading with $R = 1$. On the other hand, for an almost 90° corner turning test with $\boldsymbol{\sigma}' \cdot \dot{\boldsymbol{\varepsilon}}'$ positive but small, the above rate-independent model predicts a reduced shear modulus with $R \approx (1 - f)$. Thus, in contrast with the rate-dependent model of Sections 4 and 5, the rate-independent model of this section could predict a discontinuous change in the value of the reduction factor R when plastic loading begins.

In conclusion, the above exercise indicates essential difficulties in using the associated rate-independent theory with the yield function (59) to model the main response characteristics due to a rapid change in the direction of straining. Those difficulties are not present in the rate-dependent viscoplastic counterpart.

REFERENCES

Bodner, S. R. (1985). Evolution equations for anisotropic hardening and damage of elastic–viscoplastic materials. In *Plasticity Today—Modelling, Methods And Applications* (Edited by A. Sawczuk and G. Bianchi), pp. 471–482. Elsevier, London.

Bodner, S. R. (1987). Review of a unified elastic–viscoplastic theory. In *Unified Constitutive Equations For Creep And Plasticity* (Edited by A. K. Miller), pp. 273–301. Elsevier, London.

Bodner, S. R. (1992). A lower bound on bifurcation buckling of viscoplastic structures. *Acta Mech.* [Suppl] **3**, 181–190.

Bodner, S. R. and Partom, Y. (1972). A large deformation elastic–viscoplastic analysis of a thick-walled spherical shell. *ASME J. Appl. Mech.* **39**, 751–757.

Bodner, S. R. and Partom, Y. (1975). Constitutive equations for elastic–viscoplastic strain-hardening materials. *ASME J. Appl. Mech.* **42**, 385–389.

Bodner, S. R., Naveh, M. and Merzer, A. M. (1991). Deformation and buckling of axisymmetric viscoplastic shells under thermomechanical loading. *Int. J. Solids Structures* **27**, 1915–1924.

Budiansky, B. (1959). A reassessment of deformation theories of plasticity. *ASME J. Appl. Mech.* **26**, 259–264.

Bushnell, D. (1976). BOSOR5—program for buckling of elastic–plastic complex shells of revolution including large deflection and creep. *Comput. Structures* **6**, 221–239.

Chan, K. S., Bodner, S. R. and Lindholm, U. S. (1988). Phenomenological modeling of hardening and thermal recovery in metals. *ASME J. Engng Mater. Tech.* **110**, 1–8.

Christoffersen, J. and Hutchinson, J. W. (1979). A class of phenomenological corner theories of plasticity. *J. Mech. Phys. Solids* **27**, 465–487.

Engesser, F. (1889). Ueber die Knickfestigkeit Geradu Strabe. *Z. Architek. Ing., Hannover* **35**, 456–462.

Gerard, G. (1946). Secant modulus method for determining plate instability above the proportional limit. *J. Aeronaut. Sci.* **13**, 38–48.

Gerard, G. and Becker, H. (1957). *Handbook of Structural Stability*: Part I—*Buckling of Flat Plates*. National Advisory Committee For Aeronautics, Technical Note 3781.

Gjelsvik, A. and Lin, G. S. (1987). Plastic buckling of plates with edge frictional shear effects. *J. Engng Mech.* **113**, 953–964.

Gray, D. E. (1957). *American Institute of Physics Handbook*. McGraw Hill, New York.

Hashiguchi, K. (1993). Fundamental requirements and formulation of elastoplastic constitutive equations with tangential plasticity. *Int. J. Plasticity* **9**, 525–549.

Hutchinson, J. W. (1974). Plastic buckling. In *Advances in Applied Mechanics* (Edited by C. S. Yih), Vol. 14, pp. 67–143. Academic Press, New York.

Inoue, T. (1994). Analysis of plastic buckling of rectangular steel plates supported along their four edges. *Int. J. Solids Structures* **31**, 219–230.

Inoue, T. and Kato, B. (1993). Analysis of plastic buckling of steel plates. *Int. J. Solids Structures* **30**, 835–856.

Naghdi, P. M. and Trapp, J. A. (1975). The significance of formulating plasticity theory with reference to loading surfaces in strain-space. *Int. J. Engng Sci.* **13**, 785–797.

Needleman, A. and Tvergaard, V. (1982). Aspects of plastic postbuckling behavior. In *Mechanics of Solids* (Edited by H. G. Hopkins and M. J. Sewell), pp. 453–498. Pergamon Press, Oxford.

Ohashi, Y. and Ohno, N. (1982). Inelastic stress-responses of an aluminum alloy in non-proportional deformations at elevated temperature. *J. Mech. Phys. Solids* **30**, 287–304.

Onat, E. T. and Drucker, D. C. (1953). Inelastic instability and incremental theories of plasticity. *J. Aeronaut. Sci.* **20**, 181–186.

Rubin, M. B. (1987a). An elastic–viscoplastic model exhibiting continuity of solid and fluid states. *Int. J. Engng Sci.* **25**, 1175–1191.

Rubin, M. B. (1987b). An elastic–viscoplastic model for metals subjected to high compression. *ASME J. Appl. Mech.* **54**, 532–538.

Rubin, M. B. (1989). A time integration procedure for plastic deformation in elastic–viscoplastic metals. *J. Appl. Math. Phys. (ZAMP)* **40**, 846–871.

Rubin, M. B. (1990). Analysis of viscoplasticity in 6061-T6 aluminum. *J. Appl. Phys.* **68**, 4523–4530.

Shanley, F. R. (1947). Inelastic column theory. *J. Aeronaut. Sci.* **14**, 261–268.

Stowell, E. Z. (1948). A unified theory of plastic buckling of columns and plates. *NACA Rep.* **898**, 1–11.

Stowell, E. Z. (1951). Compressive strength of flanges. *NACA Rep.* **1029**, 1–14.

Tugcu, P. (1991). Plate buckling in the plastic range. I. *J. Mech. Sci.* **33**, 1–11.

Tvergaard, V. (1988). Plasticity and creep at finite strains. In *Theoretical and Applied Mechanics* (Edited by P. Germain, M. Piau and D. Caillerie), pp. 349–368. Elsevier, Amsterdam.